Predicting Energy Usage during Milling Based on Workpiece Properties

Hannah Budinoff

A report submitted in partial satisfaction of the
requirements for the degree of
Master of Science, Plan II
in Mechanical Engineering

at the

University of California, Berkeley

Committee in charge:
Professor David Dornfeld
Professor Lisa Pruitt

Fall 2015

Acknowledgments

This material is based upon work supported by the National Science Foundation Graduate Research Fellowship Program under Grant No. 1106400.

This work would not be possible without the support of Professor David Dornfeld and the Laboratory for Manufacturing and Sustainability. Thank you.

Special thanks to Raunak Bhinge, for his constant support and encouragement on this project.

Contents

List of Figures

List of Tables

1 Introduction

The need to understand the environmental impact of human action and to make changes to minimize this impact is of growing importance in engineering efforts. This is true especially for large industrial companies, where the large scale of operations means that business decisions can have global environmental implications. The consumption of natural resources is central to manufacturing.Manufacturing processes consume material and energy, and output a final good along with potentially hazardous byproducts. All of these inputs and outputs have potential environmental consequences.

Although the impact of raw material and processing byproducts are the currently the focus of most energy reduction efforts currently, energy usage of manufacturing is equally important. Less energy used on the shop floor means less emissions emitted at the power plant and decreased use of natural resources needed to fuel the power plants. Manufacturing is responsible for 90% of total energy consumption and 84% of CO2 emissions in the industrial sector [Schipper, 2006]. These percentages present a challenge, but also an opportunity to make significant environmental impact.

Incremental improvements in the efficiency of a manufacturing process will be multiplied many times over because the process will be used again and again to produce parts. The energy required to manufacture a given product depends on the raw material used, the manufacturing process itself, and the way that process is executed. For example, manufacturing a part by casting would require less energy than making that same part from metal powder forming because of the different energy demands of the processes [Ashby, 2012]. But the manufacturing process used typically depends on the ultimate function of the part, the ease of creating part features, the processing time, and perhaps above all, the process cost.

The work presented in this thesis focuses on improving material selection by developing a better understanding of the factors that drive energy consumption in machining. Choice of material, like choice of manufacturing process, depends on many factors, especially the desired function of the part. However, there currently is not enough research for designers to make informed decisions when considering the importance of energy consumption. A designer trying to choose between two different aluminum alloys with similar functional properties currently has no way of knowing which material would be more energy efficient. New materials also present potential challenges: it is currently difficult to estimate the energy required to machine a novel material with a particular set of properties without prior experimentation.

Improved knowledge on this topic would enable manufacturers to optimize the efficiency of their machining processes through modeling. More specifically, data collection during the machining process could be used to improve models and material selection tools for designers. If manufacturers can predict and control how much energy their parts require, they can schedule production differently to minimize energy. It would also be possible to make changes to toolpaths and materials to minimize energy consumption. Designers, too, can make changes to part material and geometry to minimize energy consumption.

This area of research also has the potential to contribute to a better understanding of tool wear. Although certain manufacturing companies are interested in the energy their processes use, it is not yet a global concern. Tool wear, on the other hand, is a global concern in industry. Manufacturers do not have a good ability to predict when a tool will wear out,

leading to unexpected downtime and lost profits. By knowing the correlation between tool wear, energy consumption, and workpiece material, manufacturers could better predict when a tool will wear out and could take actions to replace the tool, therefore avoiding downtime.

1.1 Background

1.1.1 Modeling of energy usage in machining

Previous research has been done to develop methods to predict energy consumption of milling processes. Early researchers developed empirical relationships with speeds and feed rates to estimate cutting forces and power, which helped machinists to design fixtures and determine the proper speed to use on a particular machine [DeVries, 2011]. These equations tended to be very specific to a particular tool geometry, material type, and cutting conditions, such as those developed by Boston [1941].

More recent efforts have attempted to use advances in technology to develop more general energy prediction models. Gutowski et al. developed an equation to approximate the power required for manufacturing [2006]:

$$P = P_0 + k\dot{v} \tag{1}$$

For machining, k is a constant called the specific cutting energy, $\dot{v}$ is the material removal rate, and P_0 is the energy consumption that takes place both during machining and during idling, due to processes that enable machine tool running such as the coolant pump and computer control systems.

A graphical representation of this breakdown of energy can be seen in Figure 1. P_0 is constant while the actual cutting energy varies depending on the rate at which material is removed. This representation is useful for illustrative purposes but the fraction of power consumed by the cutting process and the idle processes varies from machine to machine.

Dividing Equation 1 by the material removal rate, it is possible to calculate the energy per unit volume of material removed, or specific energy, e (not to be confused with the specific *cutting* energy, k):

$$e = \frac{P}{\dot{v}} = \frac{P_0}{\dot{v}} + k \tag{2}$$

As shown in Figure 2, Diaz et al. verified that the energy required from a cut has an inverse dependency on the material removal rate [2011]. They proposed a slightly different model for this trend:

$$e_{cut} = \frac{\kappa}{\dot{v}} + b \tag{3}$$

where e_{cut} is the specific energy, and κ and b are experimentally determined constants, which must be determined for every combination of materials and process parameters.

The model of Gutowski et al. (Equation 2) is a valid approximation but because material properties are captured in a single term, k, it lacks granularity. The model implies that the specific cutting energy is constant for any combination of cutting parameters. Further, it doesn't identify which properties or conditions are most responsible for driving up energy consumption.

The work of Diaz and others [Diaz et al., 2012; Kara and Li, 2011] has resulted in models with high accuracy but this accuracy is mostly based on the fact that the model is built

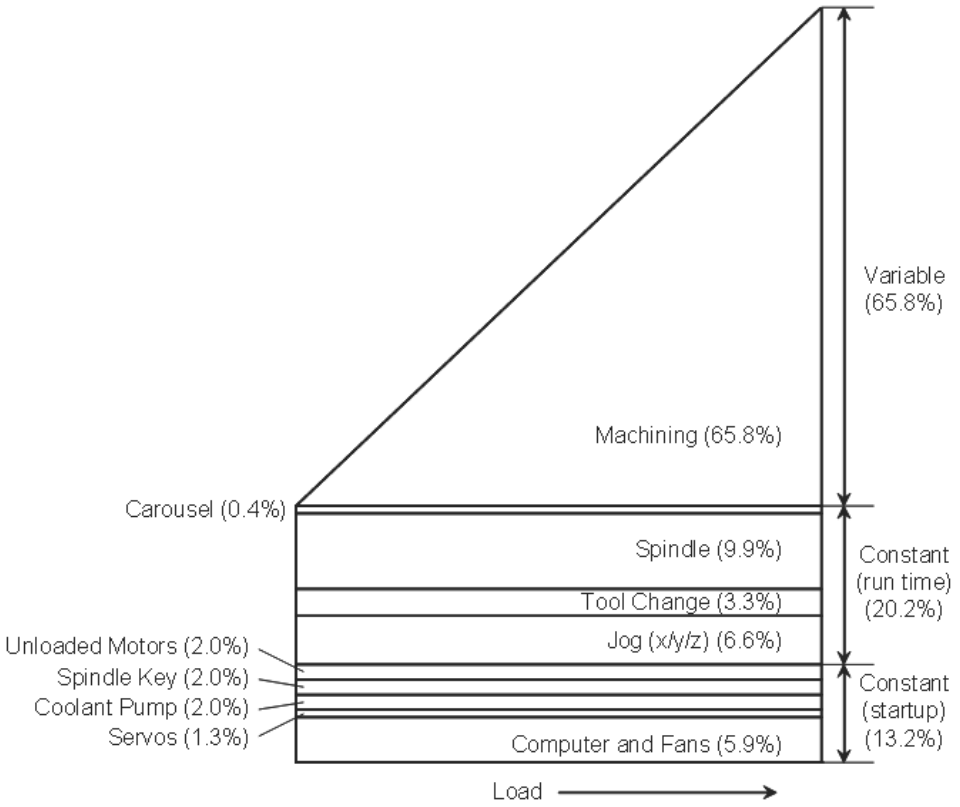

Figure 1: Graphical representation of the power consumption of a 3-axis automated milling machine [Kordonowy, 2003]

to best fit experimental data. The constants of the model would need to be determined through experimentation for different materials or cutting parameters. The major limit of this approach is its lack of general applicability. One model cannot be applied to a wide range of materials. Another limitation is that this model has little connection to the physics of the cutting process. While Gutowski's model uses specific cutting energy, an estimate of the machinability, the model parameters used in Equation 3 are unitless and are unconnected to the underlying physics of the problem. There is still a need for a granular, generally applicable, and physically meaningful model.

1.1.2 Impact of material properties on machining

One important consideration when selecting a workpiece material and corresponding cutting parameters is the concept of machinability. Machinability, the relative ease of machining a material, is a complicated concept with many different definitions and means of measurement. It is typically associated with tool life, energy required for cutting, or surface quality [Mills and Redford, 1983].

This work focuses on machinability as defined by the energy required to cut a material. The machinability of a material can be approximated by its specific cutting energy, which is the amount of energy required to remove a unit volume of workpiece material [DeVries, 2011]. The specific cutting energy for a material is largely a function of hardness [Boothroyd, 1989]

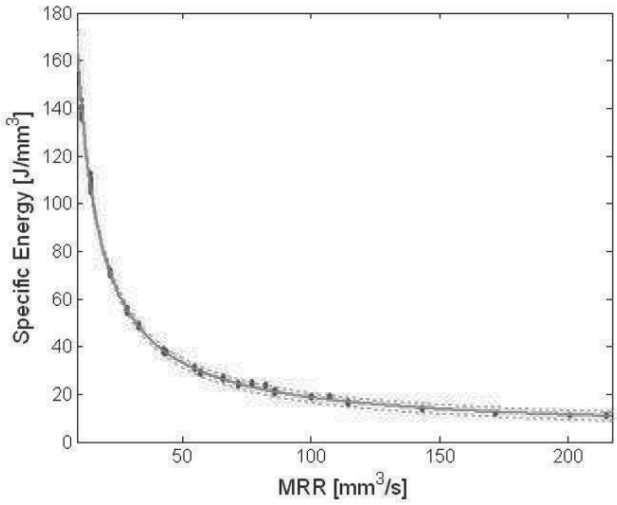

Figure 2: Relationship of cutting energy to material removal rate (MRR) [Diaz et al., 2011]

but the relationship between hardness and specific cutting energy is generally qualitative and useful only over large ranges in hardness (i.e. a hard steel will be easier to machine than a soft brass).

Specific energy values can also be estimated by cutting forces. For orthogonal machining, Kalpakjian and Schmid [2006] give the total specific energy, e_t, as the sum of the specific energy for shearing, e_s, and the specific energy for friction, e_f. Here, F_s is the shear force, V_s is the shear velocity, w is width of cut, t_0 is undeformed chip thickness, and r is the cutting ratio, equal to t_0/t where t is chip thickness.

$$e_t = e_s + e_f = \frac{F_s V_s}{w t_0 V} + \frac{Fr}{w t_0} \tag{4}$$

This equation implies that properties relating to friction and shearing are important but further insight is limited. This calculation would typically be based on experimental data of cutting forces so it does not have any clear advantage over simply measuring the cutting energy itself.

Approximate specific cutting energy, k, values are found experimentally and summarized in reference tables but the number of materials with known specific energy values is relatively small. Further, the tables frequently do not list more than one temper of a material. In the absence of specific cutting energy values for every material a designer might want to use, general predictive equations or rules of thumb, relating widely available material properties like hardness or thermal conductivity, could help designers. If designers could easily estimate the specific cutting energy for their part based on material properties that they already know, they could make more informed decisions regarding machining energy of parts.

The material properties and the condition of the workpiece directly impact the variable energy usage of machining. Specifically, properties such as modulus of elasticity, thermal conductivity, thermal expansion can impact machinability. Additional properties driven by workpiece condition, such as microstructure, grain size, heat treatment, chemical composition, fabrication, yield strength, and ultimate tensile stress can also affect machinability [Schneider, 2002]. Although these variables affect machinability, the exact relationship is un-

known. This work seeks to explore and define the relationships between material properties and machinability, as measured by energy consumption during machining.

2 Methods

2.1 Experimental Design

The long term goal of this effort is to develop a model that can accurately predict energy consumption of machining for a wide spectrum of materials. As a first step, an experiment was designed to determine the relative importance of workpiece material properties on energy consumption. This experiment was designed and executed by the author along with other members of an ME 290I semester team (Raunak Bhinge, Yumin Huang, and Maxwell Micali).

Table 1: Summary of workpiece materials

Material	Temper
Aluminum 7075	T651
Aluminum 7075	T7351
Aluminum 7075	O (Annealed)
Aluminum 7050	T7451
Aluminum 6061	T6511
Aluminum 2024	T351
Aluminum 6013	T651
Brass 360	H02
Steel A36	
Steel 1018	As cold drawn

Workpiece materials for this experiment were chosen with the goal of capturing a wide range of material properties. This goal was somewhat limited by the fact that all materials were to be machined with the same feed rates and spindle speeds, in an effort to keep some experimental variables constant. Several aluminum alloys with different tempers were selected. Choosing different tempers of the same alloy made it possible to keep some material properties constant (e.g. density and thermal conductivity) to better see the effect of the other properties (e.g. hardness and ultimate tensile strength). In addition to the aluminum alloys, free machining brass and two types of low carbon steel were selected. The selected materials are shown in Table 1.

A toolpath geometry was selected that required several different basic milling operations. A 2.5"x2.5" block of 1" thickness was machined, starting with face milling, followed by several slotting, pocketing, and drilling operations. The finished part geometry is shown in Figure 3. Cuts were made in both the x- and y-direction. A drawing showing the dimensions of each feature is shown in the appendix.

The Taguchi technique [Box et al., 2005] was used to generate a full factorial design of experiments for the cutting parameters used during milling. Four levels of chip load, three

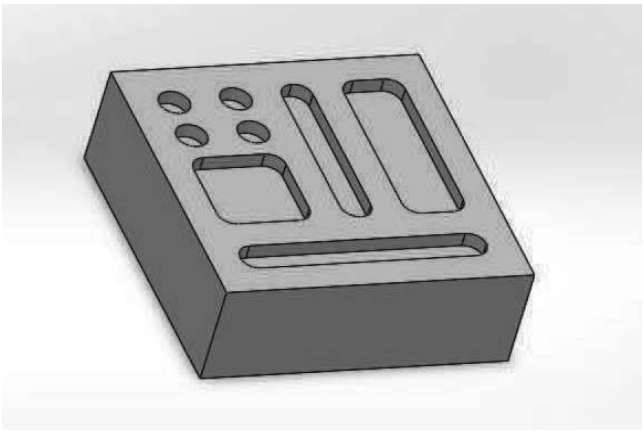

Figure 3: Geometry of finished experimental part

levels of spindle speed, and three levels a of axial depth of cut were specified. The feed rate was calculated to meet the specified levels of chip load at the three levels of spindle speed, based on the equation:

$$CL = \frac{v_f}{N n_t} \tag{5}$$

where CL is chip load per tooth, v_f is feed rate, N is number of teeth on the cutter, and n_t is the spindle speed in RPM.

Both climb and conventional cuts were used. The feed rates and spindle speeds were chosen to be appropriate for the wide range of materials selected in this experiment.

Part 1 had an axial depth of cut of 1 mm for all operations, Part 2 had a depth of cut of 0.5 mm, and Part 3 had a depth of cut of 1.5 mm. The series of operations, feed rates, and spindle speeds were identical across all three parts and for each material.

A Mori Seiki NV1500 DCG Machining Center equipped with power monitoring sensors was used for this experiment. Previous work showed that this machine did not require significantly more amount of energy to make cuts in the x- or y-direction. The total machine power was measured at a frequency of 100 Hz. Energy usage of each cut was calculated as the integral of power and duration of the cut. The MTConnect standard [Vijayaraghavan and Dornfeld, 2010] was used for collecting and archiving sensor data and machine operation information (such as speeds and loads). This allowed us to track the energy usage, duration, feed rate, spindle speed, depth of cut, and other variables for each machining operation.

The tool used for these experiments was a $\frac{1}{4}$" 4-flute solid carbide square end-mill with TiN coating. The tool was replaced for each part to prevent tool wear from impacting the data. Coolant was used throughout the milling process.

2.2 Data Analysis

Data collected during experiments was post-processed following the procedure described in Bhinge et al. [2014]. Because of the way the data was post-processed, each cut specified in the G-code (the numerical control programming language used to specify the toolpath) was treated as an independent data point. This enabled us to break down each feature into a

series of energy consumption data points, each with a particular duration, feed rate, and spindle speed. The speed and feed were constant for each cut but changed between cuts.

The data was filtered to only include cutting operations longer than 2 seconds to eliminate shorter cuts which tended to have more variation in the measured energy usage. All operations that did not involve actual cutting were filtered out. Plunge with feed cuts (with the exception of drilling operations) were excluded as well.

In order to validate the experimental data, the specific cutting energy, k, was calculated. Following Equation 2, the specific cutting energy was calculated by finding the linear least squares regression for the specific energy (calculated as the ratio of energy [J] and volume removed [mm^3] for each cut) and the inverse of the material removal rate (calculated from the volume removed and duration [s] of each cut). Using the inverse of the material removal rate allowed for the use of a simple linear regression, with the specific cutting energy, k, estimated by the y-intercept, and the constant non-cutting power term, P_0, estimated by the slope.

After making the decision to analyze the data according to Equation 1, the drilling operations were excluded from further analysis because pecking was used. The time spent raising the tool rapidly up and down was included in the time duration of the cut so, strictly speaking, the reported time reflected more than cutting time. The other feature types (facing, slotting, and pocketing) were included in one regression. The range of MRR was wide, from approximately 0.1 to 450 mm^3/s for the Part 1 (depth of cut equal to 1 mm). The average material removal rate for Part 1 was approximately 25 mm^3/s. As seen in Figure 4a, most of the data for Part 1 was between 10 and 30 mm^3/s. Because depth of cut is used to calculate the MRR, the range and average of the MRR was different for each depth of cut but the results of Part 1 alone are presented for the sake of simplicity.

To examine the effects of feed rate and spindle speed, the data was filtered and regressions were found to calculate k for only data with a particular feed rate and spindle speed. To avoid analyzing regressions that were insignificant due to lack of data points, k was calculated only when more than 8 cuts with the particular feed rate and spindle speed, with duration greater than 2 seconds, were identified. For all toolpaths, these criteria were only met at three combinations of speed and feed, summarized in Table 2.

Feed rate [mm/s]	Spindle speed [rpm]	Chip load [mm]
152.3	1500	0.0254
304.6	1500	0.0508
304.6	3000	0.0254

Table 2: Summary of usable feed and speed combinations, after filtering

3 Results

The results are grouped into several topics: Influence of material removal rate; calculation of specific cutting energy; influence of depth of cut and other cutting parameters; relationships

between material properties and energy usage; and discussion of a dimensionless parameter to predict energy usage.

3.1 Influence of material removal rate

The specific energy was found to have an inverse relationship to the material removal rate (MRR), as seen in Figure 4. Our results agree with previous findings [Diaz et al., 2012; Kara and Li, 2011] as well with Equation 2, which shows an inverse dependence on the MRR.

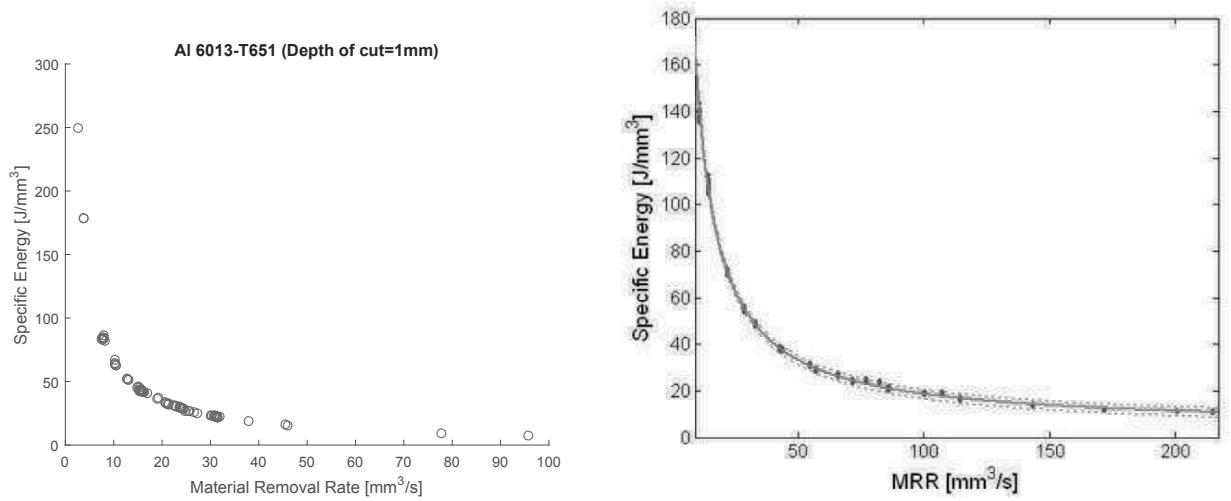

(a) (b)

Figure 4: Comparison of (a) experimental results with (b) published results from Diaz et al. [2011]

This relationship is evident over a wide range of MRRs and cutting operations. Figure 4a includes facing, slotting, and pocketing operations but the data can all be described by the inverse relationship. This relationship will be shown in more detail in the subsequent section.

3.2 Calculation of specific cutting energy

Plots summarizing the regression are presented in Figures 5 though 9. Plots representing a depth of cut of 1 mm are shown in the body of the text. Plots for a depth of cut of 0.5 mm and 1.5 mm are included in the appendix. The few data points of cuts with extremely low material removal rates exerted a strong influence on the regression line. This can seen in Figure 6 and 8, where negative values of k were calculated. To avoid the effect of these few data points, a second linear regression was calculated for each part and material. The second regression limited the data to material removal rates less than 5 mm^3/s (i.e. 0.2 s/mm^3). This range was chosen because it captured the majority of the data while eliminating the extreme values which were heavily influencing the regression.

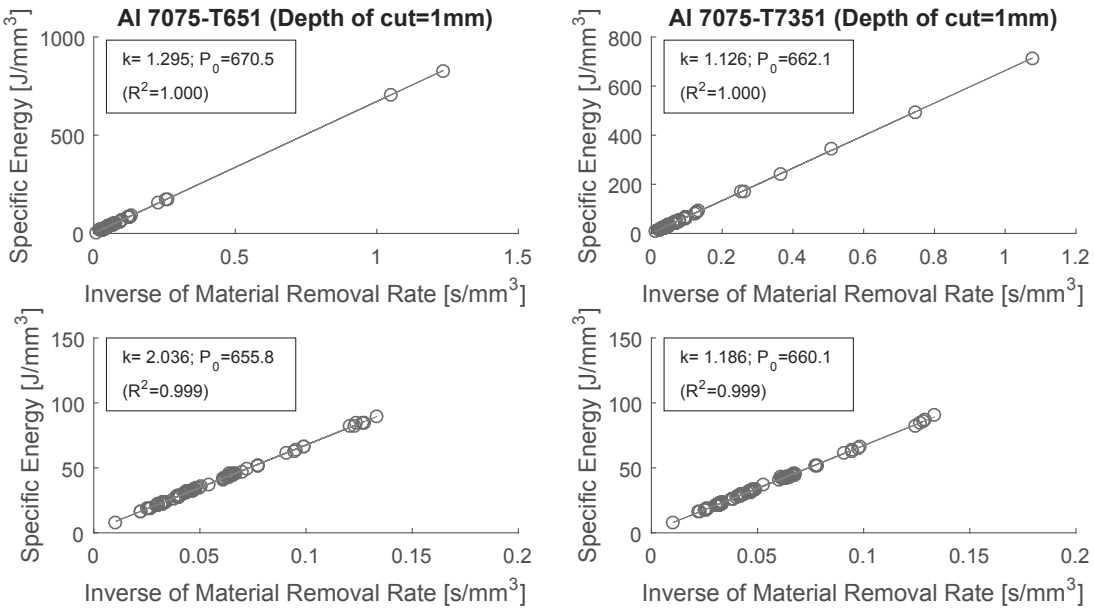

Figure 5: Relationship of specific cutting energy and inverse of material removal rate for 7075-T651 and 7075-T7351 (Depth of cut =1mm). Upper plots include all data while lower plot only includes $MRR^{-1} < 0.2$.

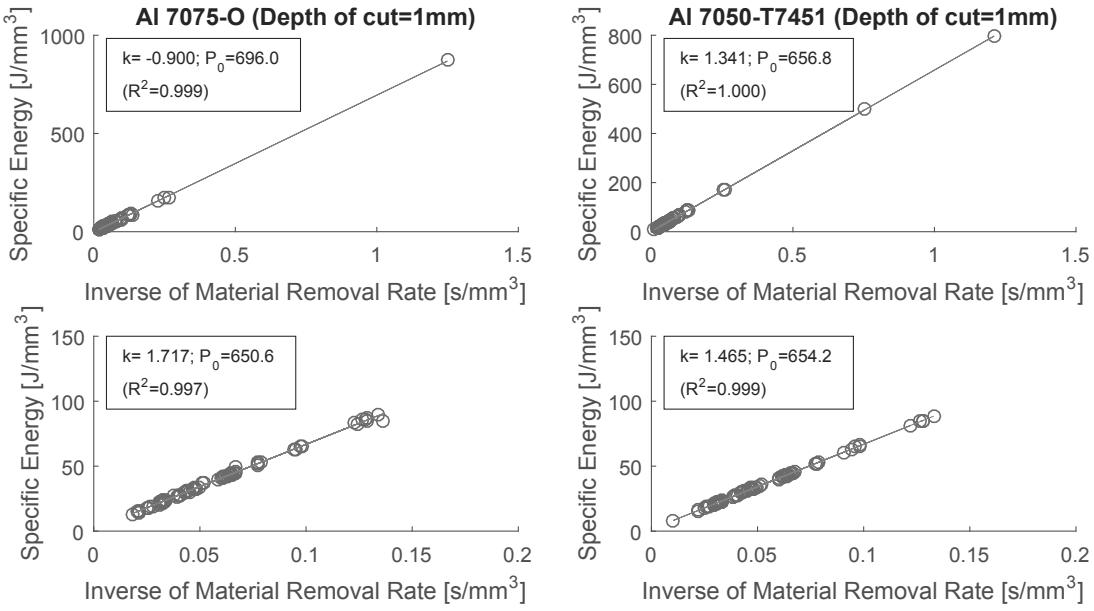

Figure 6: Relationship of specific cutting energy and inverse of material removal rate for 7075-O and 7050-T7451 (Depth of cut =1mm). Upper plots include all data while lower plot only includes $MRR^{-1} < 0.2$.

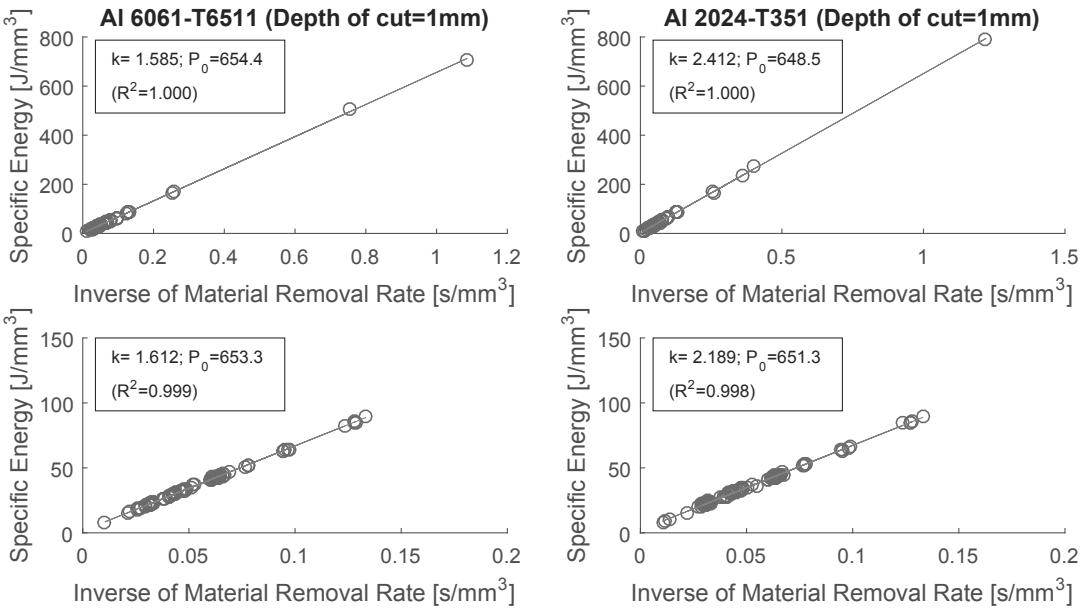

Figure 7: Relationship of specific cutting energy and inverse of material removal rate for 6061-T6511 and 2024-T351 (Depth of cut =1mm). Upper plots include all data while lower plot only includes $MRR^{-1} < 0.2$.

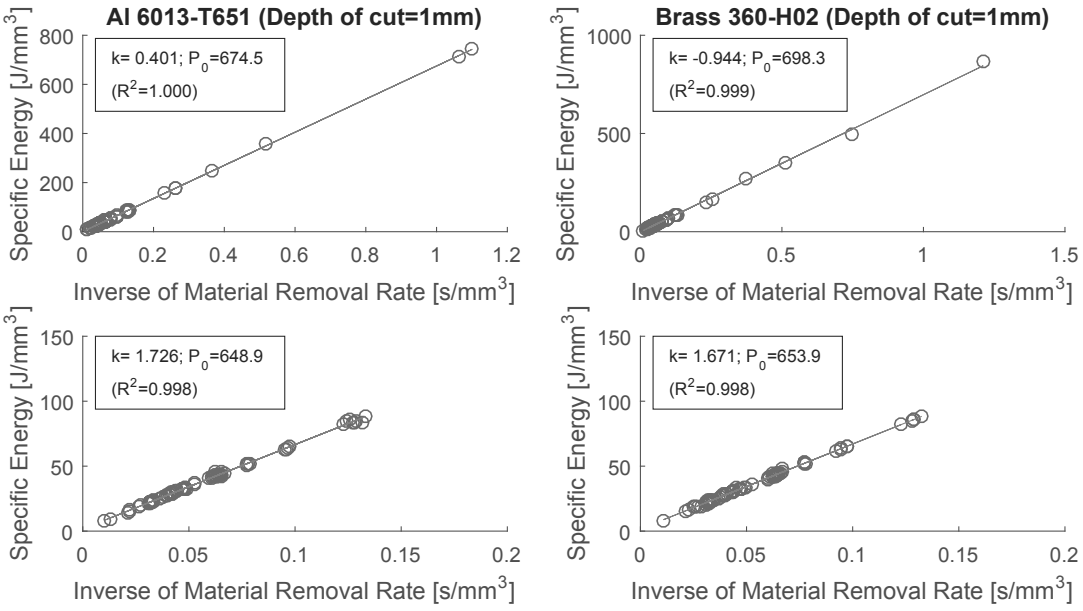

Figure 8: Relationship of specific cutting energy and inverse of material removal rate for 6013-T651 and Brass 360-H02 (Depth of cut =1mm). Upper plots include all data while lower plot only includes $MRR^{-1} < 0.2$.

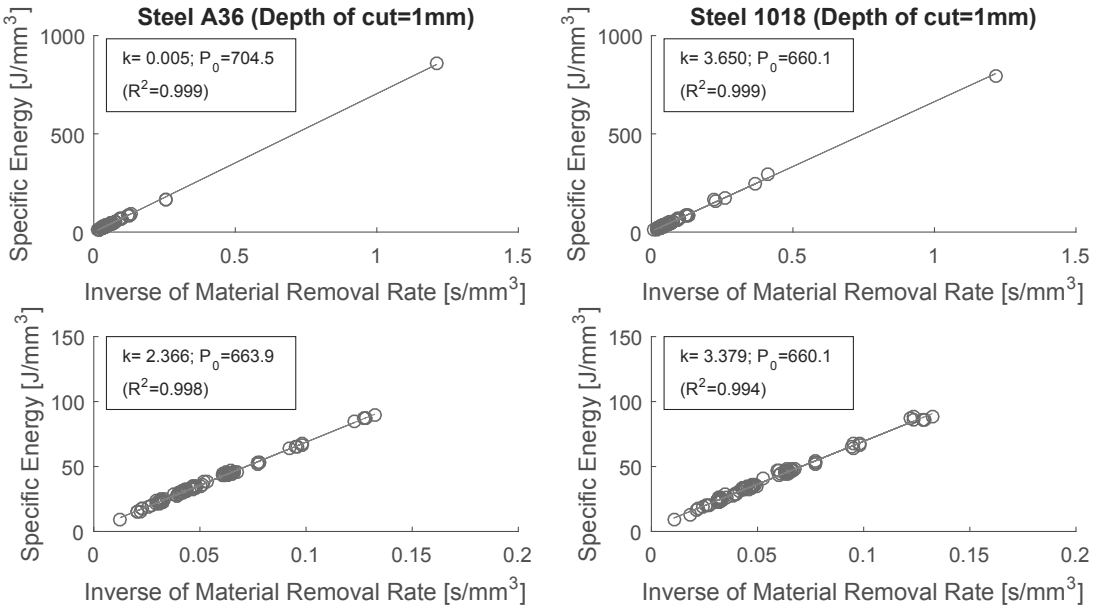

Figure 9: Relationship of specific cutting energy and inverse of material removal rate for A36 and 1018 (Depth of cut =1mm). Upper plots include all data while lower plot only includes $MRR^{-1} < 0.2$.

Material	k (Depth of cut=0.5 mm) [J/mm^3]	k (Depth of cut=1 mm) [J/mm^3]	k (Depth of cut=1.5 mm) [J/mm^3]
Aluminum 7075-T651	2.914	2.036	0.728
Aluminum 7075-T7351	2.712	1.186	0.774
Aluminum 7075-O	2.013	1.717	1.713
Aluminum 7050-T7451	2.670	1.465	1.216
Aluminum 6061-T6511	2.522	1.612	1.437
Aluminum 2024-T351	4.048	2.189	1.612
Aluminum 6013-T651	2.713	1.726	0.891
Brass 360-HO2	1.492	1.671	0.999
Steel A36	3.347	2.366	1.362
Steel 1018	3.686	3.379	2.883

Table 3: Comparison of experimental specific cutting energy, k, values for each depth of cut

The lowest calculated coefficient of determination (R^2) was 0.952 for all depths of cut calculated from data where $MRR^{-1} < 0.2$. Table 3 summarizes the values of k calculated from the least squares regression for the data with $MRR^{-1} < 0.2$, as shown in the lower half of Figures 5 through 9. The values of k vary with depth of cut.

P_0 which represents the non-cutting power, is roughly constant for all of the regressions using the same toolpath and depth of cut. The average P_0 is 656.2 W and the relative standard deviation is 0.66%, based on the regressions where $MRR^{-1} < 0.2$ and depth of cut is 1 mm. For a depth of cut of 0.5 mm, the average P_0 is 649.2 W and the relative standard deviation is 1.04%. For a depth of cut of 1.5 mm, the average P_0 is 665.75 W and the relative standard deviation is 1.84%.

Material	Published k [J/mm^3]
Aluminum 6061-T6511 *	0.76
Aluminum alloys †	0.4-1
Steel A36 *	2.5
Steel 1019 *	2.07
Steels †	2-9
Brass 360-H02 *	0.68
Copper alloys †	1.4-3.2

*[DeVries, 2011]; †[Kalpakjian and Schmid, 2006]

Table 4: Published specific cutting energy values.

Table 4 summarizes some published values of specific cutting energy. Specific cutting energy is often given as a range of values so those ranges are presented along with a few relevant values for particular materials.

3.3 Influence of depth of cut and other cutting parameters

Cuts were made in both the climb and conventional directions but the results did not indicate that one direction consistently required significantly more energy in comparison to the other direction. Both climb and conventional cuts are included in the plots shown in the previous section and both were used to find the regressions.

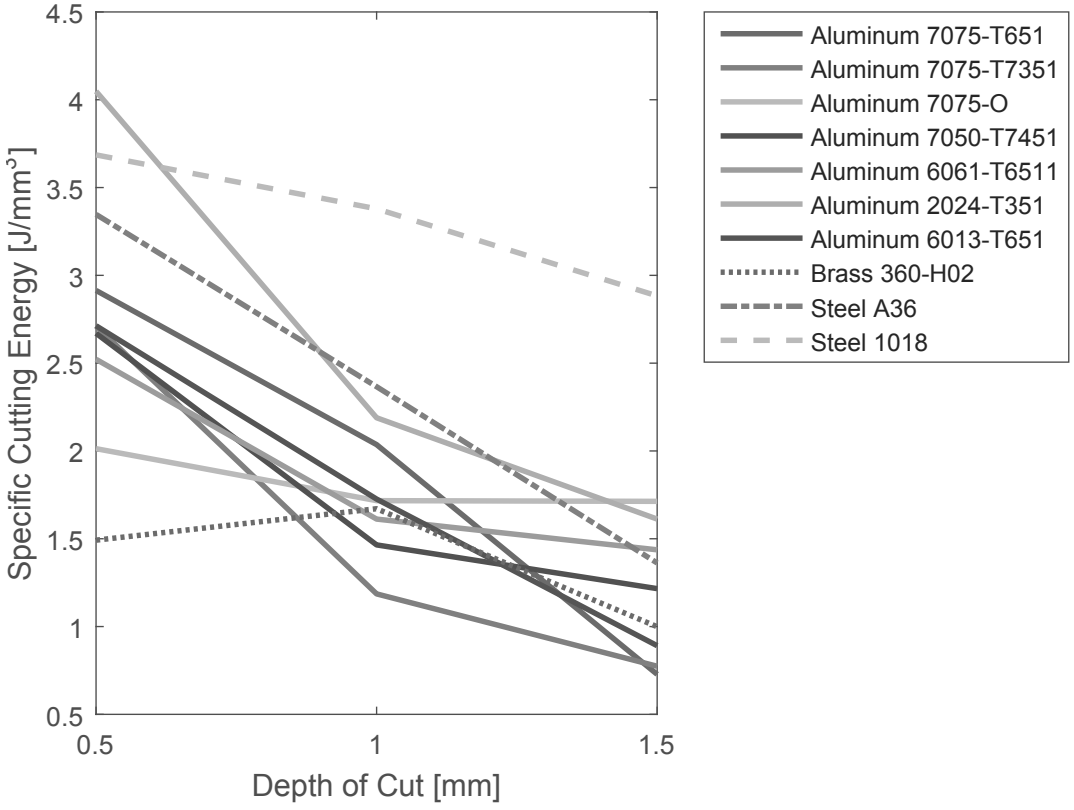

Figure 10: Specific cutting energy, k, has a decreasing relationship to axial depth of cut

As shown in Figure 10, the calculated k exhibited a dependence on axial depth of cut. For most materials, increases in depth of cut tended to lead to decreases in k. For Aluminum 7075-O and Brass 360-H02, k did not decrease for each depth of cut but the k calculated for a depth of cut of 0.5 mm was the higher than the k calculated for a depth of cut of 1.5 mm.

As discussed in the Section 2.2, drilling was excluded from data analysis because pecking was used. Some published values of specific cutting energy provide different values for drilling versus face milling [Todd et al., 1994]. The values of k provided by Todd et al. are higher for milling than for drilling.

3.4 Relationships between material properties and energy usage

Common properties, as well as properties linked to machinability, were gathered for the experimental materials. Most values were taken from the ASM Handbook, especially Volumes 1 and 2 [ASM International, 1990]. Toughness was approximated as the product of

Specific cutting energy, k [J/mm^3]									
	Depth of cut=0.5mm			Depth of cut=1mm			Depth of cut=1.5mm		
Material	Set A	Set B	Set C	Set A	Set B	Set C	Set A	Set B	Set C
Al 7075-T651	1.40	1.81	2.28	2.51	0.65	0.60	0.39	1.33	1.74
Al 7075-T7351	1.04	1.89	3.15	0.61	1.37	2.00	0.30	1.21	1.47
Al 7075-O	3.10	0.19	2.63	2.12	1.46	1.60	1.89	1.92	2.11
Al 7050-T7451	1.38	1.70	2.94	1.01	1.53	1.40	1.38	0.59	0.91
Al 6061-T6511	1.33	1.96	2.55	1.17	1.49	1.23	0.83	1.87	1.76
Al 2024-T351	3.63	2.49	3.62	0.94	1.83	2.81	1.18	1.22	0.60
Al 6013-T651	1.90	0.42	1.85	2.28	0.29	0.51	0.67	0.33	0.69
Brass 360	1.22	0.01	2.78	2.55	1.23	1.55	0.71	1.46	1.40
Steel A36	1.47	2.97	4.91	1.92	4.21	2.91	2.06	1.05	2.52
Steel 1018	5.35	0.48	1.48	5.48	2.57	2.81	2.76	4.54	2.71

Table 5: Calculated k values for all three depths of cuts and different combinations of feed rate and spindle speed. Set A: 1500 RPM, 152.3 mm/s; Set B: 1500 RPM, 304.6 mm/s; Set C: 3000 RPM, 304.6 mm/s

measured hardness and published values of percent elongation. To determine the relative impact of these material properties on the energy usage of the cutting process, represented by the specific cutting energy, simple linear regressions were calculated. Material properties for each material were plotted against the specific cutting energy of that material, for each depth of cut. The coefficient of determination for all researched material properties is shown in Table 6.

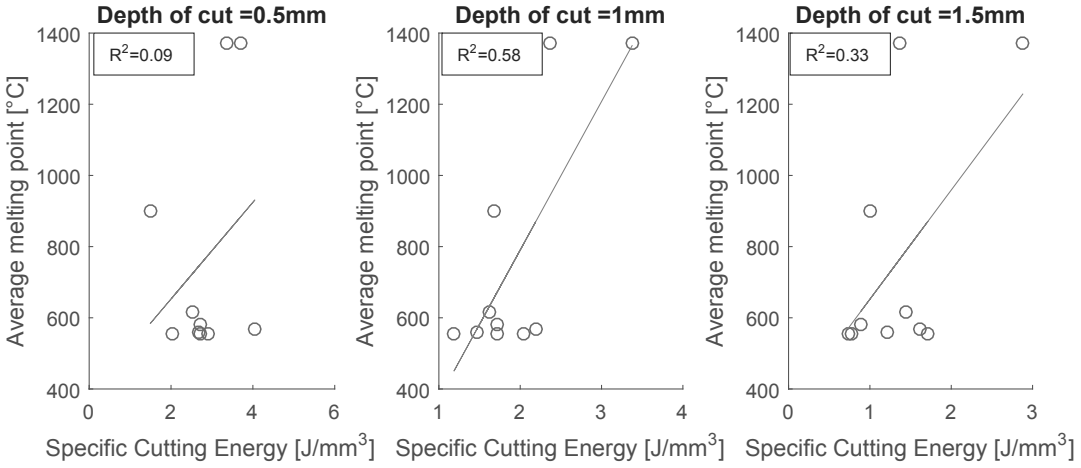

Figure 11: Specific cutting energy, k, tends to increase for materials with higher melting points

The material properties which had the highest coefficient of determination for all three depths of cut are plotted in Figures 11 through 14. Thermal properties (i.e. average melting point and thermal conductivity) tended to be more related to the specific cutting energy for higher depths of cut (1 and 1.5 mm). Strength properties (i.e. UTS and hardness) tended

Material Property	R^2 for depth of cut=0.5 mm	R^2 for depth of cut=1 mm	R^2 for depth of cut=1.5 mm
Average coefficient of thermal expansion [μm/m·°C]	0.01	0.12	0.03
Average melting point [°C]	0.09	0.58	0.33
Thermal conductivity at 25 C [W/m·K]	0.19	0.61	0.32
Density [g/cm^3]	0.00	0.32	0.15
Modulus of elasticity [MPa]	0.17	0.65	0.39
Ultimate tensile strength [MPa]	0.27	0.03	0.05
Ultimate shear stress [MPa]	0.21	0.00	0.11
Tensile yield strength [MPa]	0.10	0.00	0.10
Theoretical hardness (HRB)	0.26	0.07	0.02
Measured hardness (HRB)	0.41	0.06	0.00
Elongation in 50 mm [%]	0.04	0.20	0.15
Area reduction [%]	0.08	0.03	0.06
Strain hardening exponent [MPa]	0.26	0.01	0.08
Approximation of toughness (product of hardness and % elongation)	0.61	0.36	0.07

Table 6: Coefficient of determination, R^2, for studied material properties and specific cutting energy values of each experimental material. Area reduction value was unavailable for 6013-T651.

to be more related to the specific cutting energy for lower depths of cut (0.5 and 1 mm).

If the steel and brass data were excluded from the regression, the property which resulted in the highest coefficient of determination is the approximation of toughness (the product of measured hardness and published values of percent elongation).

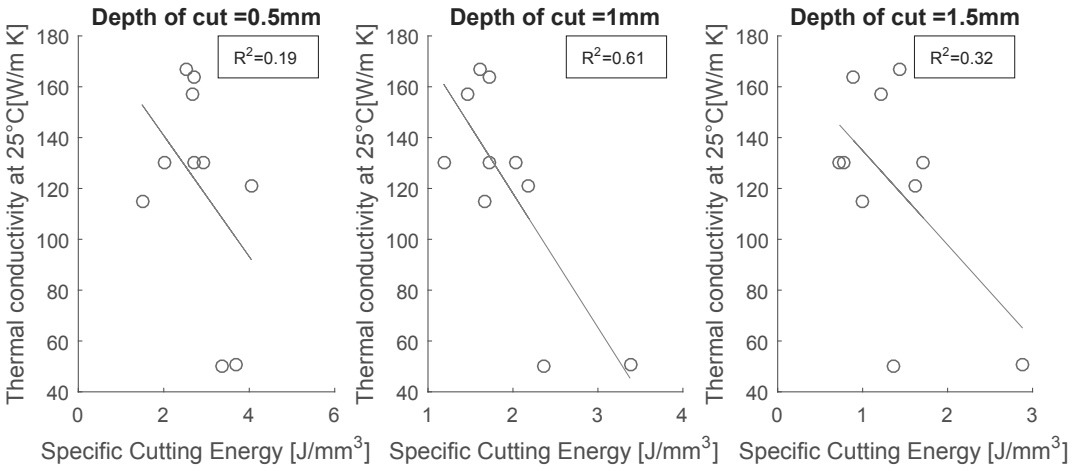

Figure 12: Specific cutting energy, k, tends to be lower for materials with high thermal conductivity

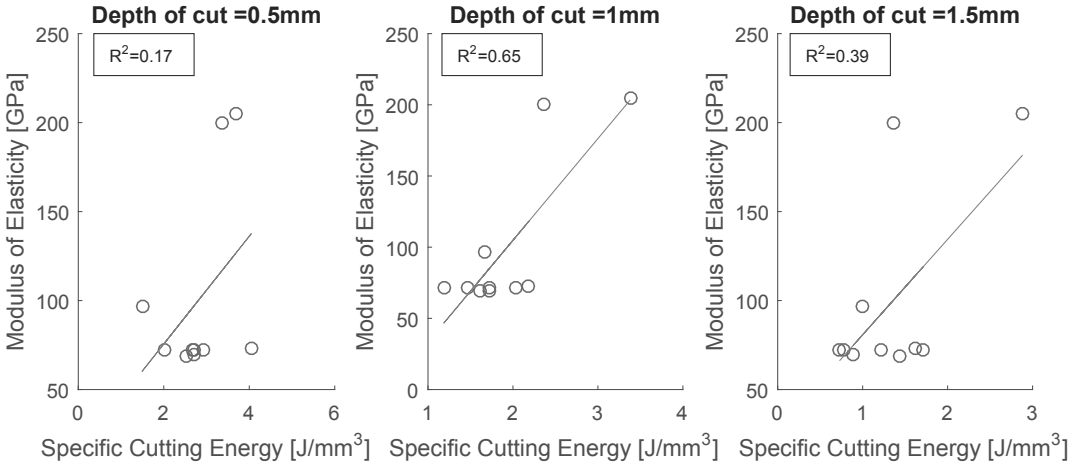

Figure 13: Specific cutting energy, k, is higher for materials with a high modulus of elasticity

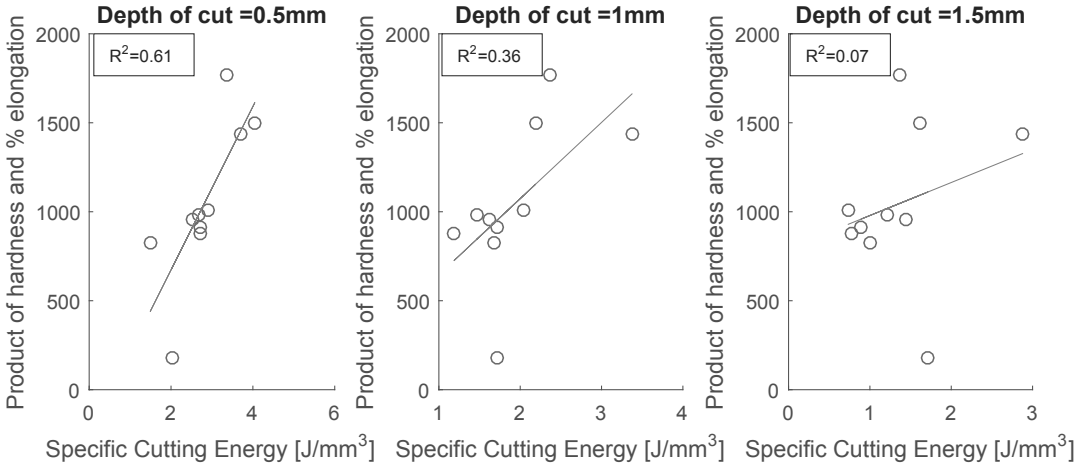

Figure 14: Specific cutting energy, k, tends to be higher for materials with a large product of hardness and percent elongation

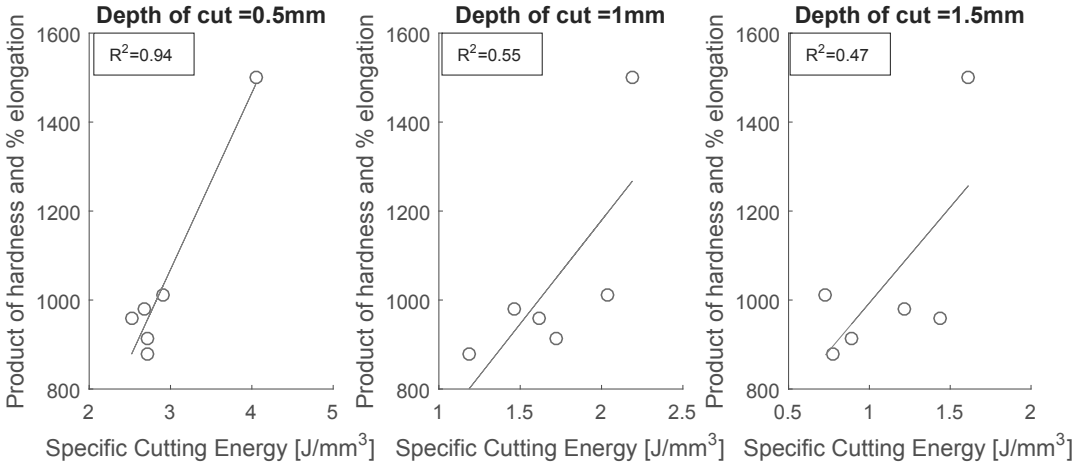

Figure 15: When restricted to aluminum (excluding Al 7075-O, which appeared to have a different behavior when machined than the other aluminums,) specific cutting energy, k, tends to be higher for materials with a large product of hardness and percent elongation

3.5 Dimensionless parameter to predict energy usage

Previous research has examined the influence of a variety of physical properties on machinability [Henkin and Datsko, 1963; Janitzky, 1944; Boulger et al., 1951]. Interestingly, Henkin and Datsko built an esimate for machinability based on similar material properties to the ones found to be significant in this study. The basis of their analysis was the development of dimensionless groups describing the machining process, summarized in Equation 6. Here, the area ratio R_f is a measure of ductility; h and w are depth and width of cut, respectively; α is thermal diffusivity; Θ is temperature; H_B is Brinell hardness; ρC is volume specific heat; and J is the mechanical equivalent of heat. The subscript x indicates a particular tool life (i.e. when x=60, this indicates cutting speed that results in a 60-minute tool life) and the corresponding interface temperature.

$$(\frac{v_x w}{\alpha})(h/w)^a = (\frac{J\rho C\Theta_x}{H_B})^b (R_f)^c \tag{6}$$

Grouping the cutting parameters and temperature (assumed constant) into a single constant, A_2; replacing $\alpha\rho C$ with its equivalent, λ, thermal conductivity; and replacing R_f with the more common measure of ductility, area reduction (A_r), Equation 6 can be reduced to:

$$v_{60} = \frac{A_2\lambda}{H_B}(1 - A_r/100)^{1/2} \tag{7}$$

The cutting speed that results in a 60-minute tool life, v_{60}, is chosen by Henkin and Datsko as an estimate of the machinability of a workpiece material. Because specific cutting energy can be used as an approximation of machinability, this relationship is interesting and possibly relevant to our work. Figure 16 shows regressions for the v_{60} of the experimental materials, assuming A_2=1. This constant would need to be calculated for actual predictions but was not needed to plot simple regressions. The coefficient of determination is relatively low for all depths of cut but is higher than the coefficients calculated based on single material properties, shown in the previous section.

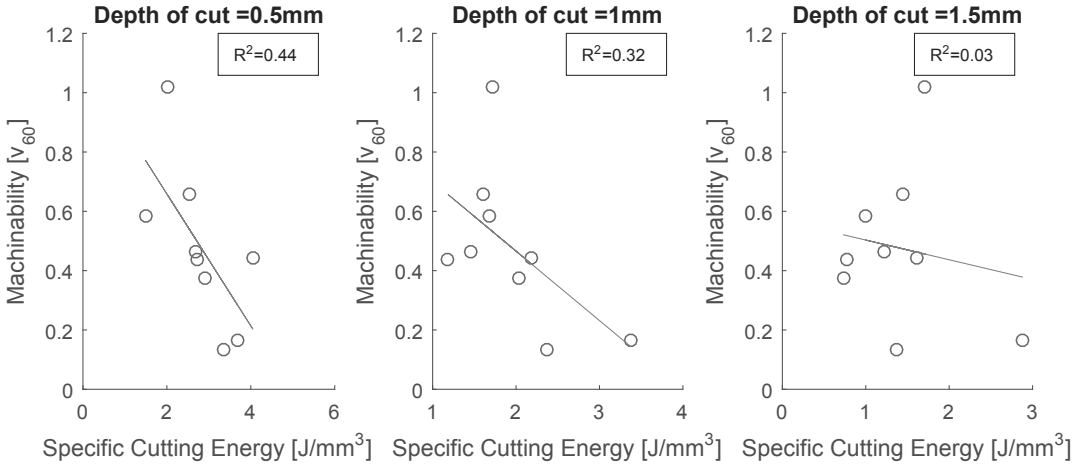

Figure 16: Specific cutting energy, k, is lower for materials with a high machinability paramater

4 Discussion

The experimental results presented in this work confirm the general validity of Gutowski's model for the specific energy of milling. The high coefficient of determination for all regressions (the lowest calculated R^2 was 0.952 for all depths of cut) show that, as represented in Equation 2, the energy usage of milling per volume removed is linearly related to the inverse of the material removal rate. Although the high R^2 values are striking, the relationship that the plots represent make basic sense. On a per unit volume basis, the plots are simply showing that cuts with higher duration [s] require more energy [J]. The slope of this line is the power demand of the milling machine. The slope, which is the P_0 term in Equation 1, should be constant for a particular toolpath, independent of workpiece material. The experimental results show that the P_0 was approximately constant for all materials machined with the same toolpath. This provides further validation of the Gutowski model.

Although the linear model does describe the data well, the values of k which were calculated from the regressions were very sensitive to data filtering. The calculated k was heavily influenced by points with low MRR (large MRR^{-1}), so the accuracy of this experiment would be improved by including more cuts with low MRR and more completely covering the range of MRR values. The values of k calculated in this work do generally agree with published values of specific cutting energy, but there are significant differences. Our experimental values of k for 6061-T6511 were found to be almost twice that reported by DeVries [2011].

The discrepancy between experimental values and published values of k is possibly due to the difference in cutting speed and feed rate. Orthogonal cutting experiments to measure specific cutting energy are typically run at "standard cutting cutting conditions" with standard tooling [DeVries, 2011]. The tables of published values do not indicate the cutting conditions used so it is not possible to validate if our experimental cutting conditions were similar. This would not necessarily present a problem if k is constant regardless of cutting conditions and tool geometry but our results indicate that that is not the case.

Specific cutting energy has actually been found to be affected by cutting speed, feed rate, tool geometry, and other factors [Boothroyd, 1989]. Our experimental results showed that k has a strong dependence on depth of cut, as seen in Figure 10. Boothroyd presents a similar result with undeformed chip thickness which is shown in Figure 17b. This relationship shows that decreases in the thickness of the chip results in increases in specific cutting energy. This is because more energy is needed to overcome the increased friction between the tool and chip [Boulger, 1990].

However, for face milling, the mean undeformed chip thickness, $a_{c_{av}}$, is not calculated from the axial depth of cut. Instead, it is calculated from the feed speed, v_f, number of teeth on the cutter, N, and spindle speed, n_t [Boothroyd, 1989].

$$a_{c_{av}} = \frac{v_f}{N n_t} \tag{8}$$

The data was filtered to evaluate k using two values of mean undeformed chip thickness, 0.0254 mm and 0.0508 mm, with a spindle speed of 1500 RPM. This data is plotted in Figure 17a. The data is somewhat noisy because only two data points were used to plot each line. Also, there was a limited amount of data used to calculate k at the two mean undeformed chip thickness values due to data filtering. Typically data from 10-20 cuts was used to calculate

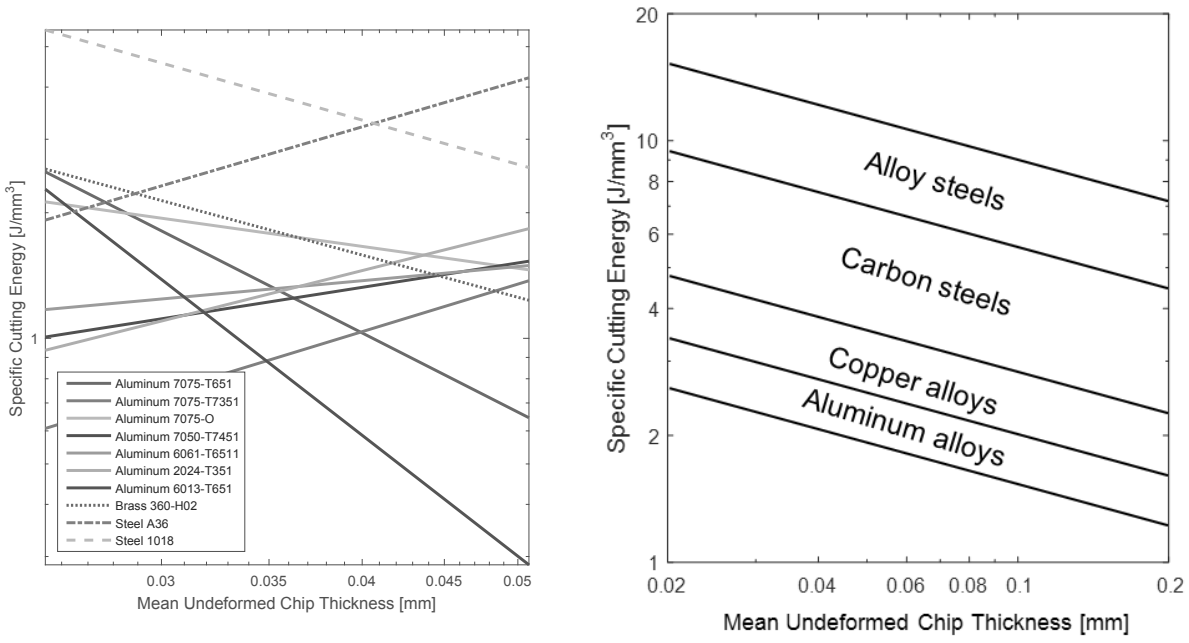

(a) (b)

Figure 17: Comparison of (a) experimental results with (b) literature relationships showing specific cutting energy decreasing with increasing undeformed chip thickness (after Boothroyd [1989])

k. These data issues could be causing the poor similarity to 17b. Another possibility is that our experimental results do not confirm the relationship reported by Boothroyd.

Boothroyd states that specific cutting energy depends on speeds and feeds [Boothroyd, 1989]. The values of k summarized in Table 5 show that different k values were calculated for different combinations of feed and speed but the relationship is unclear. Again, this lack of obvious relationship may be caused by data issues. The calculation of k is very sensitive and data issues caused by noise could be negatively impacting the calculation. More data would need to be collected to verify the relationship between chip thickness and specific cutting energy.

Another possible issue with our experimental data is the relatively low feed rate. The highest feed rate used was less than 1 m/s. Boothroyd also states that if the tool rake is held constant, specific cutting energy tends to reach a constant value at high speeds and large feeds [1989]. This can be seen graphically in Figure 18. It is possible that the calculations of k were not consistent with published results because the feed rate was too low. More experiments with higher values of feed rate would need to be run to evaluate Boothroyd's observations and to find more consistent values of k.

Other factors could be impacting specific cutting energy. Only one type of tool was used in this experiment, so the effect of tool geometry was not explored. However, Boulger [1990] states that the cutting tool geometry and material, as well as the use of coolants, do not significantly impact the specific cutting energy.

The dependency of k on cutting parameters is the main weakness of the simple Gutowski

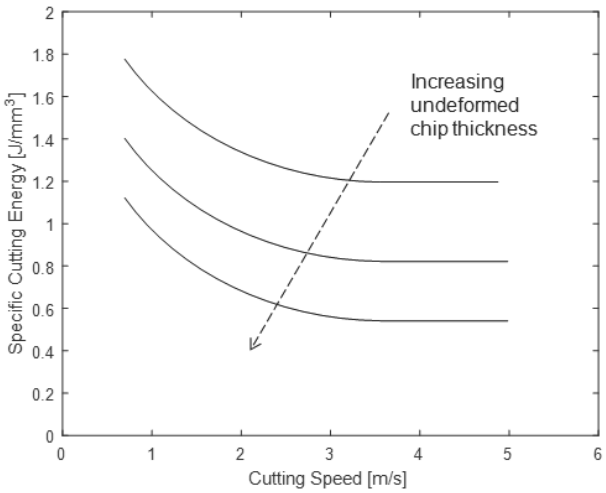

Figure 18: Specific cutting energy becomes constant at high cutting speeds (after Boothroyd [1989])

model. This model, as represented by Equation 2, assumes k is a constant for all cutting conditions. Our experimental results and other published literature invalidate this assumption. A more robust factor is needed to represent the workpiece material properties, independent of feed, speed, and cutting geometry, would be needed for a precise model for milling. Ideally, this factor would be material specific and could be multiplied by cutting parameters like speed, feed, and depth of cut, to replace the k in Equation 2.

The difficulty of calculating a constant value of specific cutting energy limited the accuracy of identifying relationships between energy usage and material properties. Another issue was that almost all material properties used in the regressions were values from published literature. These published values are based on averages of many samples of each material and are potentially a poor representation of the actual properties of the materials we machined. Material properties, like hardness, UTS, and virtually every other property, depend on the processes used to produce the material and can vary widely from batch to batch and supplier to supplier. The inaccuracy of the material properties used in our correlations is likely another source of error.

The material properties that tended to have the most distinct relationships with specific cutting energy were thermal conductivity, modulus of elasticity, and toughness (approximated as the product of hardness and percent elongation). However, these relationships were very noisy and typically not consistent across all depths of cut. Even when the data set was restricted to aluminum values only, the relationships were still not impressive. High toughness was the best predictor of k but the average coefficient of determination value for all three depths of cut was 0.65 which does not conclusively indicate that a linear relationship exists.

Further literature review after the experiments revealed that previous attempts to predict machinability based on material properties were also met with limited success. Boulger et al. found that for steels of the same type, hardness was a very poor predictor of machinability as measured by a lathe test Boulger et al. [1949]. Hardness is a better predictor when the

range in hardness is very large, as seen in Figure 19.

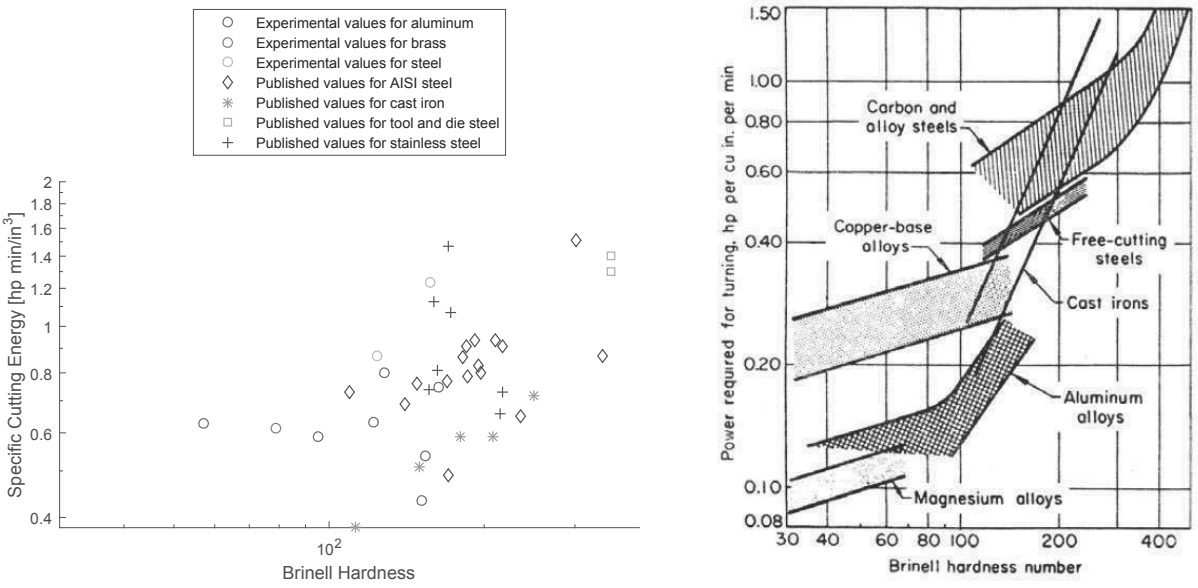

(a) (b)

Figure 19: Comparison of (a) experimental results and published results with (b) qualitative plot showing relationship of specific cutting energy to hardness [Thiele et al., 1990],

The relationship between hardness and specific cutting energy seems to be different for each set of materials, such as aluminum or carbon steel. It may be difficult to use hardness as a predictor for energy usage between or within these material groups. As shown in Figure 19b, there is a wide range of specific cutting energy values possible for a particular type of material with a specific Brinell hardness number.

Boulger [1951] determined that for similar alloys, small variations in chemical composition and microstructure played the most important role in predicting machinability. There was no attempt in our work to characterize the chemical composition or microstructure of the tested alloys. An attempt to quantify differences in cutting energy based on variations in composition and microstructure would be an interesting area of future work. There were not enough samples of a particular alloy tested in this work to pursue this direction using current experimental data.

Although three tempers of 7075 aluminum were used in this experiment, there are few conclusive findings about the influence of heat treatment. The data for the annealed 7075 aluminum was very noisy which made drawing conclusions from the data difficult. This could be due to the poor machinability of annealed aluminum. Although it is very soft, annealed aluminum 7075 has a very low machinability rating. According to the ASM Metals Handbook Desk Edition [1998], this is because the "soft, gummy" annealed material develops chips with built-up edges.

The central issue of this experiment was whether or not the cutting process can be adequately described by one or two properties. Further literature review reveals that a simple predictor for cutting energy may be difficult. The mechanics of cutting varies widely

for different materials. Microstructure and composition can have a large impact, as can thermal properties such as melting point, which results in local softening of the workpiece material. Room temperature properties were used in this work but these properties do not adequately describe the material at the elevated temperatures seen in metal cutting.

5 Conclusions and Future Work

The data from this study was very useful in confirming the validity of Gutowski's model for specific energy of machining. The high R^2 values for the regressions of specific energy and the inverse of the material removal rate indicate that Equation 2 is valid. One possible use for this model is its use for evaluating substitute materials. If energy usage is measured for a particular toolpath and toolpiece material, P_0 would be obtained. If a published value of k for the substitution candidate material was available, the energy for new part with the new material could be found.

The calculated specific cutting energy was heavily influenced by points with low MRR (large MRR^{-1}), so the accuracy of this experiment would probably be improved by including more cuts with low MRR and more completely covering the range of MRR values. More parts for each material and depth of cut would also need to be made to reduce the uncertainty and variability of the experimental values of k. The toolpath used should be modified to include to better determine the effect of speed and feed on k, as well.

The relationships between specific cutting energy and room temperature properties found in this work were not significant. In future work, it would be desirable to use more measured material properties to perform the regressions, rather than relying on published values. Hardness was measured and found to be different than published values for several materials; this discrepancy would likely occur for other properties as well. Including more materials with a wide range in hardness would also be beneficial.

To further explore the utility of re-purposing the dimensionless parameter proposed by Henkin and Datsko [1963] as a predictor for specific energy, more experimentation would be needed, especially for materials with a melting point above 600°F. It would be interesting to determine if the machinability parameter they proposed can predict specific cutting energy and if the poor fit found with our experimental data was only due to the fact that room temperature, not elevated, properties were used to calculate v_{60}. However, if elevated material properties are required for this parameter, its usefulness is somewhat limited. Like specific cutting energy, high temperature properties are not widely available for all materials.

Another interesting research direction is the link between machinability, energy usage, and tool wear. If a relationship between energy and tool wear, perhaps measured by the v_{60} parameter of Henkin and Datsko, could be found, this would provide insight into how tool wear and energy usage are linked. A link between workpiece material properties, energy usage (which can be easily monitored), and tool life would certainly be interesting to industry. Although this relationship is desirable, it might be difficult to obtain. Boulger stated that specific cutting energy "cannot be easily correlated with tool life" because tool life is heavily influenced by tool geometry and tool interactions with the workpiece part, which have a small impact on energy consumption [Boulger, 1990].

Although the experimental design and lack of repeated measurements limited the utility of

the experiential data, the findings described here can lead to better informed experimentation in the future. Our results show that k appears to be influenced by axial depth of cut as well as spindle speed and feed rate. These influences need to be studied in more detail before k should be used to represent the influence of a workpiece's material properties in a model. This work has also shown that it is very difficult to accurately represent a workpiece's behavior under all cutting conditions with only one or two material properties. A better understanding of the underlying physics of metal cutting is likely the best way to develop a model for energy prediction.

Hopefully, with future refinements and experimentation, a predictive model could be built to estimate energy consumption and perhaps tool wear. The inconclusive results of this study are best used as a reference to guide future work. Hardness still is likely the best indicator of specific energy usage because it is easily measured and does give a good estimate over a large range of materials. Charts like Figure 19b can guide designers when estimating values of k. Toughness, estimated as the product of hardness and percent elongation, may also be a useful variable to examine. In addition to the existing published tables, designers and manufacturers can make rough approximations about energy consumption. More precise estimates will require further investigation.

References

Ashby, M. (2012). *Materials and the Environment*. Elsevier LTD, Oxford.

ASM International (1990). *ASM Handbook*, 10th edition.

ASM International (1998). *Metals Handbook Desk Edition*. p. 141-149.

Bhinge, R., Biswas, N., Dornfeld, D., Park, J., Law, K., Helu, M., and Rachuri, S. (2014). An intelligent machine monitoring system for energy prediction using a Gaussian process regression. In *Big Data (Big Data), 2014 IEEE International Conference on*, pages 978–986.

Boothroyd, G. (1989). *Fundamentals of Metal Machining and Machine Tools*. Marcel Dekker, Inc, 3rd edition.

Boston, O. (1941). *Metal Processing*. John Wiley and Sons, Inc.

Boulger, F. W. (1990). Machinability of steels. *ASM International, Metals Handbook. Tenth Edition.*, 1:591–602.

Boulger, W., Moorhead, H., and Gavey, T. (1951). Superior machinability of mx steel explained. *Iron Age*, 67:90–95.

Boulger, W., Shaw, M., and Johnson, H. (1949). Constant pressure lathe test for measuring the machinability of free-machining steels. *Trans. ASME*, 71:431–438.

Box, G. E. P., Hunter, J. S., and Hunter, W. G. (2005). *Statistics for Experimenters*. Wiley John + Sons.

DeVries, W. R. (2011). *Analysis of Material Removal Processes*. Springer.

Diaz, N., Ninomiya, K., Noble, J., and Dornfeld, D. (2012). Environmental impact characterization of milling and implications for potential energy savings in industry. *Procedia CIRP*, 1:518–523.

Diaz, N., Redelsheimer, E., and Dornfeld, D. (2011). Energy consumption characterization and reduction strategies for milling machine tool use. In *Glocalized Solutions for Sustainability in Manufacturing*, pages 263–267. Springer.

Gutowski, T., Dahmus, J., and Thiriez, A. (2006). Electrical energy requirements for manufacturing processes. In *13th CIRP international conference on life cycle engineering*, volume 31.

Henkin, A. and Datsko, J. (1963). The influence of physical properties on machinability. *Journal of Manufacturing Science and Engineering*, 85(4):321–327.

Janitzky, E. (1944). Machinability of plain carbon, alloy and austenitic (non-magnetic). steel and its relation to yeld-stress ratios when tensile strengths are similar. *Trans. ASME*, 66.

Kalpakjian, S. and Schmid, S. R. (2006). *Manufacturing engineering and technology*. Pearson-Prentice Hall, 5 edition.

Kara, S. and Li, W. (2011). Unit process energy consumption models for material removal processes. *CIRP Annals-Manufacturing Technology*, 60(1):37–40.

Kordonowy, D. N. (2003). *A power assessment of machining tools*. PhD thesis, Massachusetts Institute of Technology.

Mills, B. and Redford, A. (1983). *Machinability of Engineering Materials*. Kluwer Academic Publishers Group.

Schipper, M. (2006). Energy-related carbon dioxide emissions in u.s. manufacturing. Technical report, U.S. Energy Information Administration.

Schneider, G. (2002). *Cutting Tool Applications*. Nelson Publishing.

Thiele, E. W., Kundig, K. J. A., Murphy, D. W., Saloway, G., and Duffin, B. (1990). Comparative machinability of brasses, steels and aluminum alloys: CDA's universal machinability index. In *SAE Technical Paper Series*. SAE International.

Todd, R. H., Allen, D. K., and Alting, L. (1994). *Manufacturing processes reference guide*. Industrial Press Inc.

Vijayaraghavan, A. and Dornfeld, D. (2010). Automated energy monitoring of machine tools. *CIRP Annals-Manufacturing Technology*, 59(1):21–24.

6 Appendix

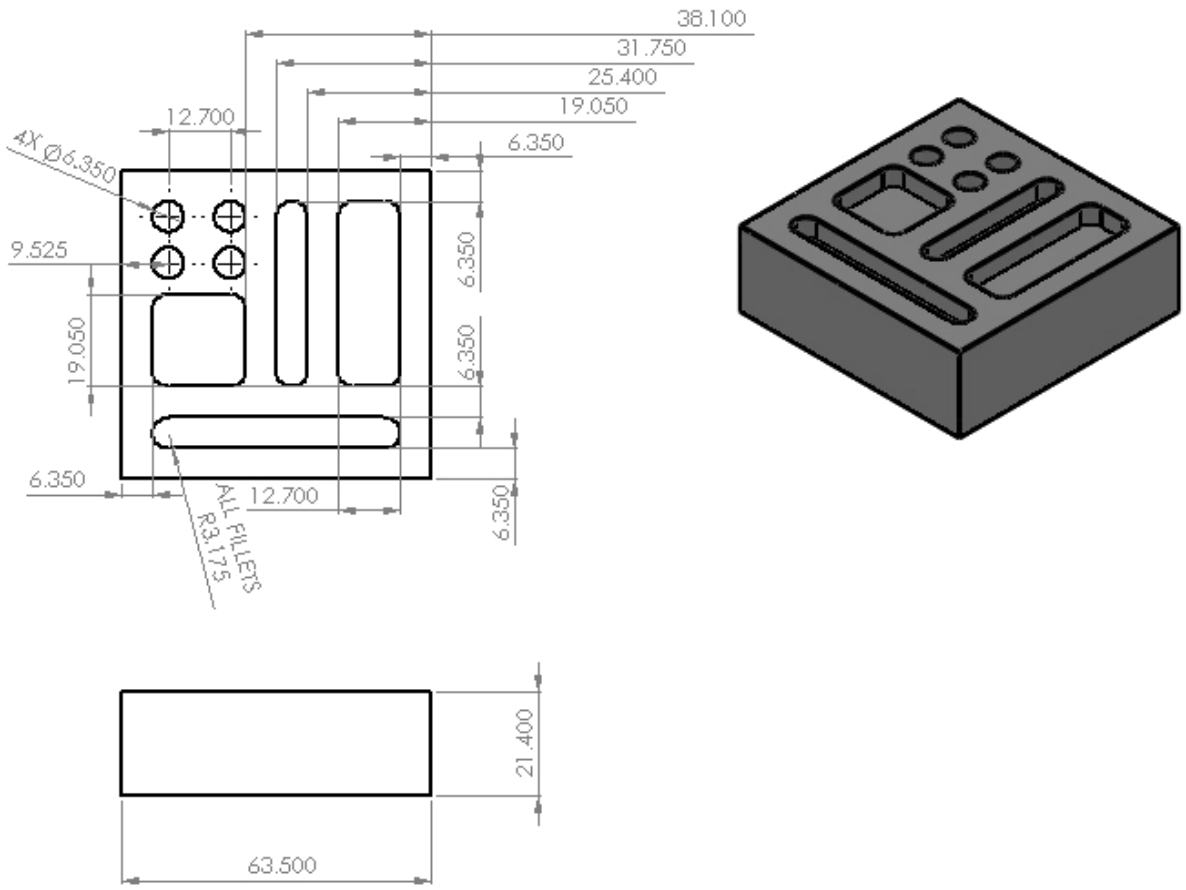

Dimensions for features of the experimental part (units are mm)

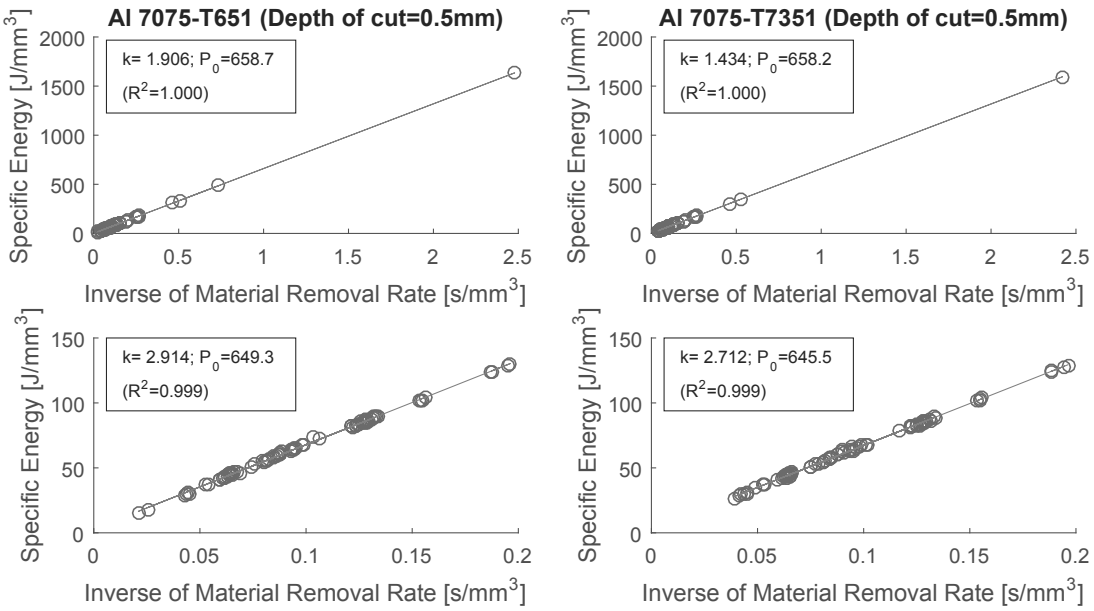

Relationship of specific cutting energy and inverse of material removal rate for 7075-T651 and 7075-T7351 (Depth of cut =0.5mm). Upper plots include all data while lower plot only includes $MRR^{-1} < 0.2$.

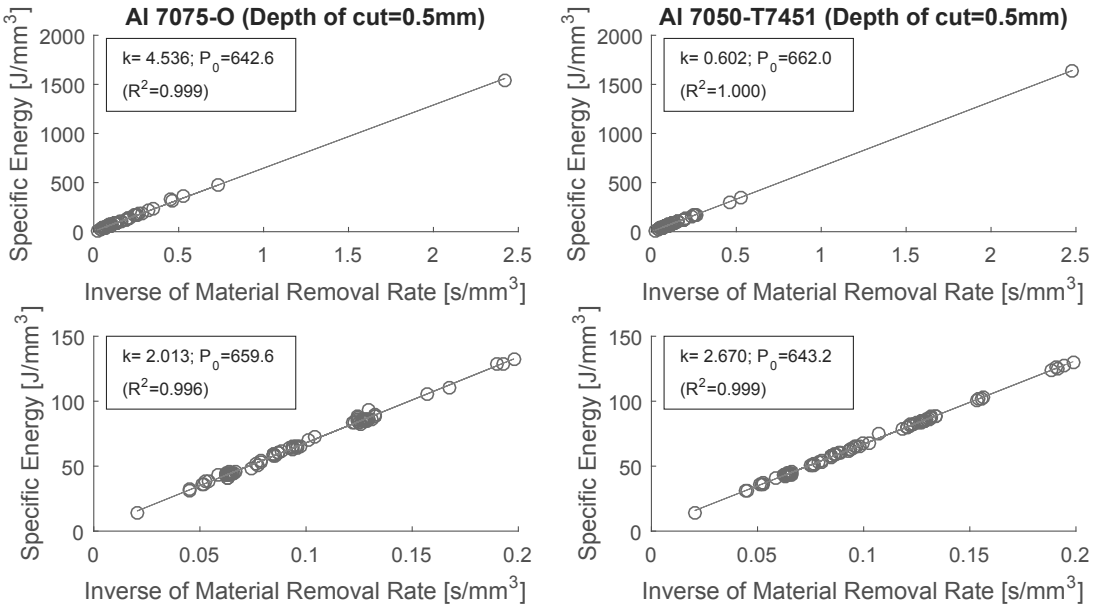

Relationship of specific cutting energy and inverse of material removal rate for 7075-O and 7050-T7451 (Depth of cut =0.5mm). Upper plots include all data while lower plot only includes $MRR^{-1} < 0.2$.

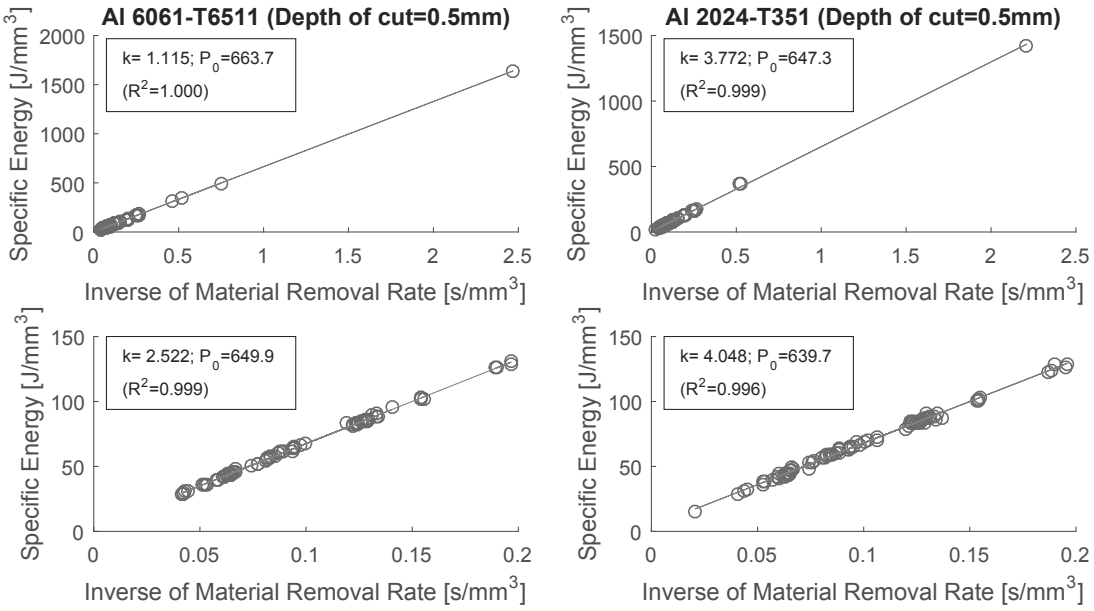

Relationship of specific cutting energy and inverse of material removal rate for 6061-T6511 and 2024-T351 (Depth of cut =0.5mm). Upper plots include all data while lower plot only includes $MRR^{-1} < 0.2$.

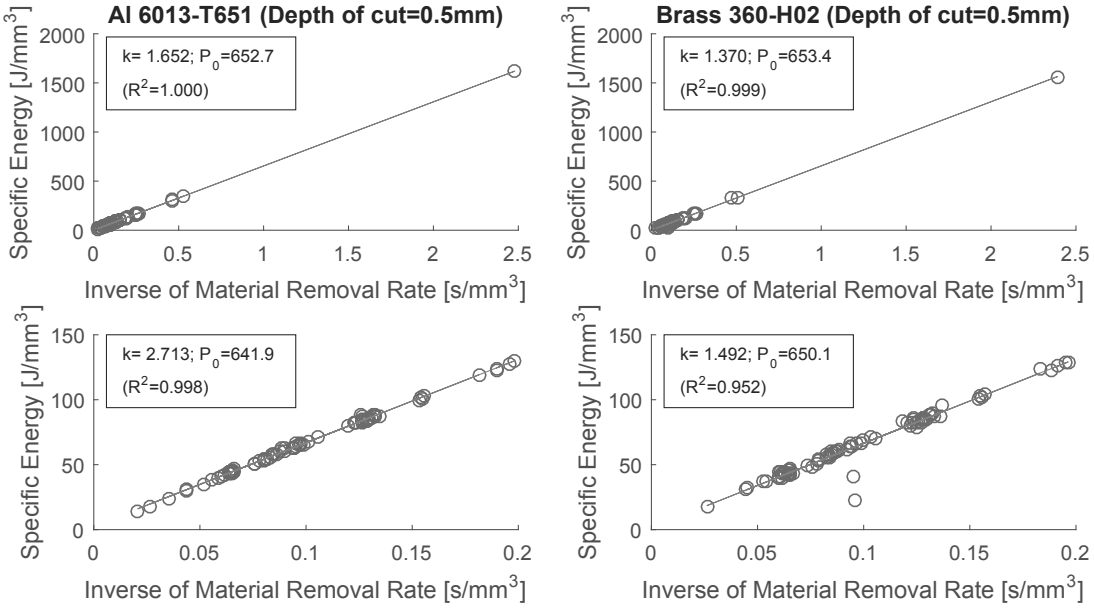

Relationship of specific cutting energy and inverse of material removal rate for 6013-T651 and Brass 360-H02 (Depth of cut =0.5mm). Upper plots include all data while lower plot only includes $MRR^{-1} < 0.2$.

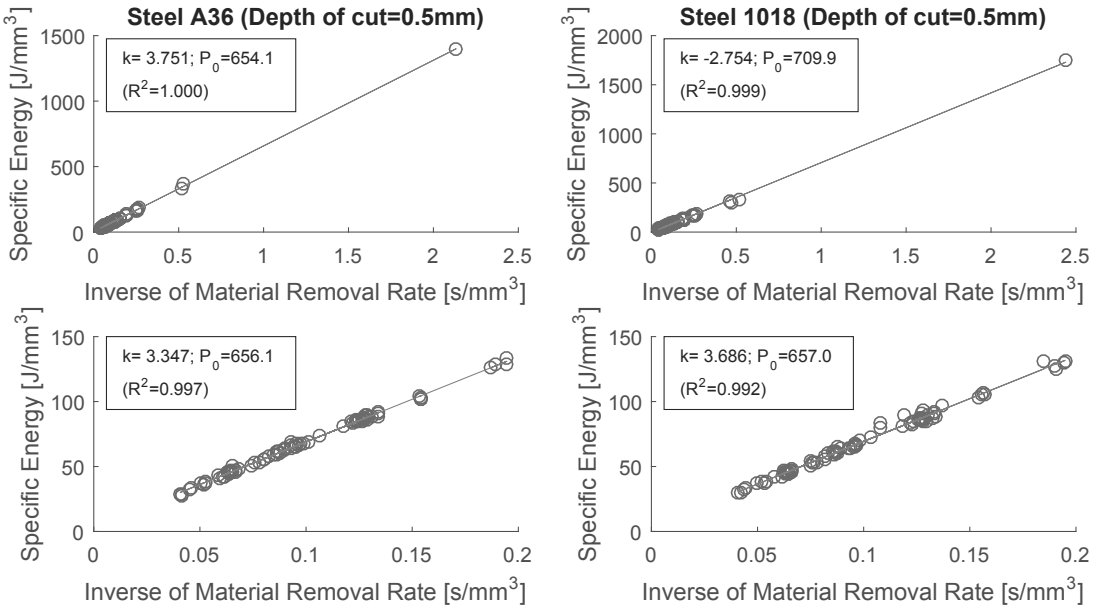

Relationship of specific cutting energy and inverse of material removal rate for A36 and 1018 (Depth of cut =0.5mm). Upper plots include all data while lower plot only includes $MRR^{-1} < 0.2$.

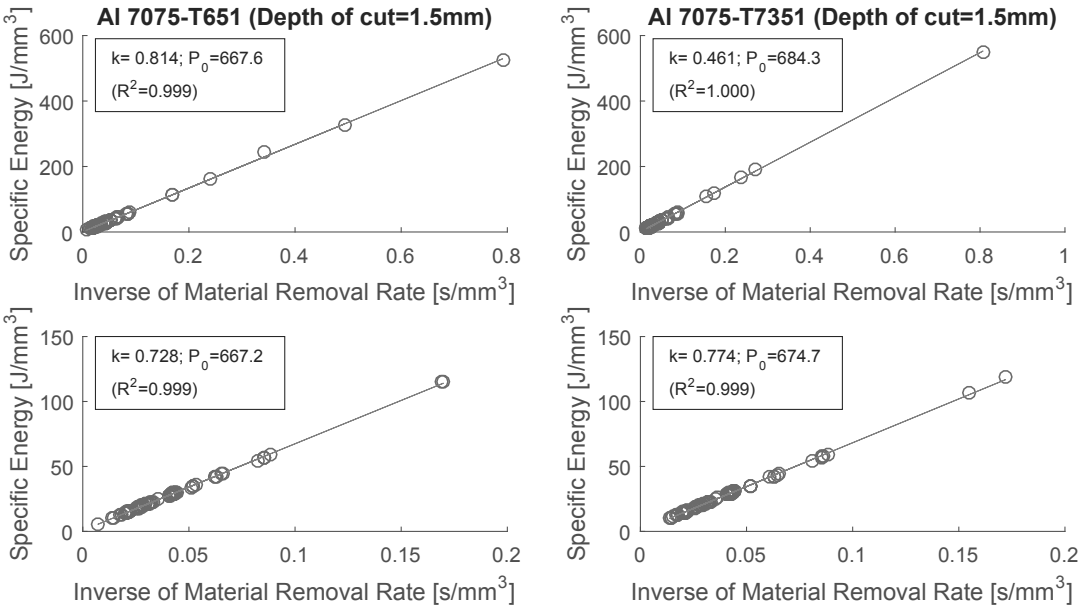

Relationship of specific cutting energy and inverse of material removal rate for 7075-T651 and 7075-T7351 (Depth of cut =1.5mm). Upper plots include all data while lower plot only includes $MRR^{-1} < 0.2$.

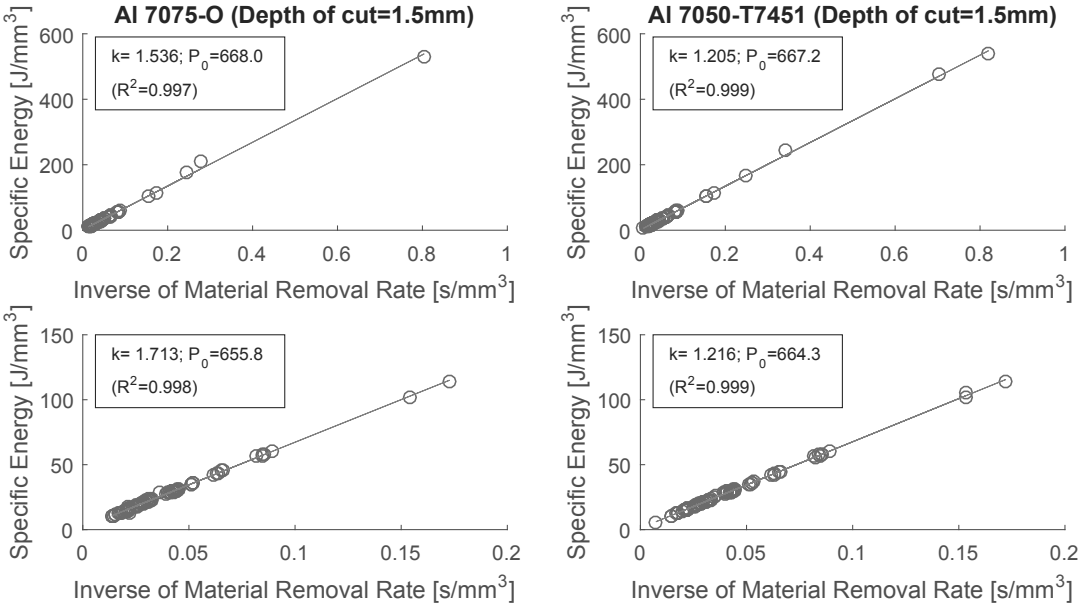

Relationship of specific cutting energy and inverse of material removal rate for 7075-O and 7050-T7451 (Depth of cut =1.5mm). Upper plots include all data while lower plot only includes $MRR^{-1} < 0.2$.

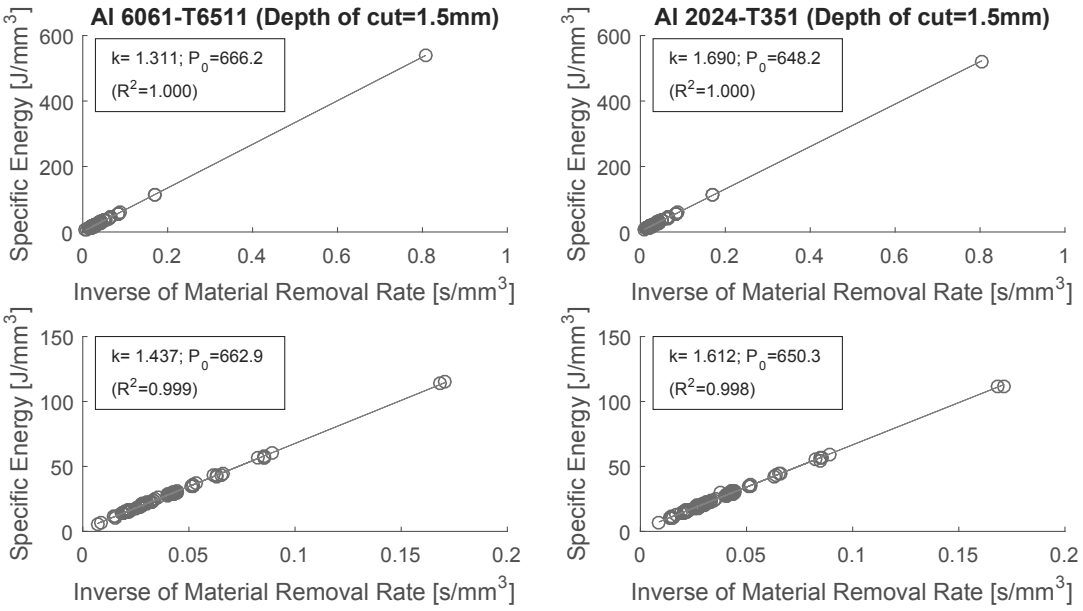

Relationship of specific cutting energy and inverse of material removal rate for 6061-T6511 and 2024-T351 (Depth of cut =1.5mm). Upper plots include all data while lower plot only includes $MRR^{-1} < 0.2$.

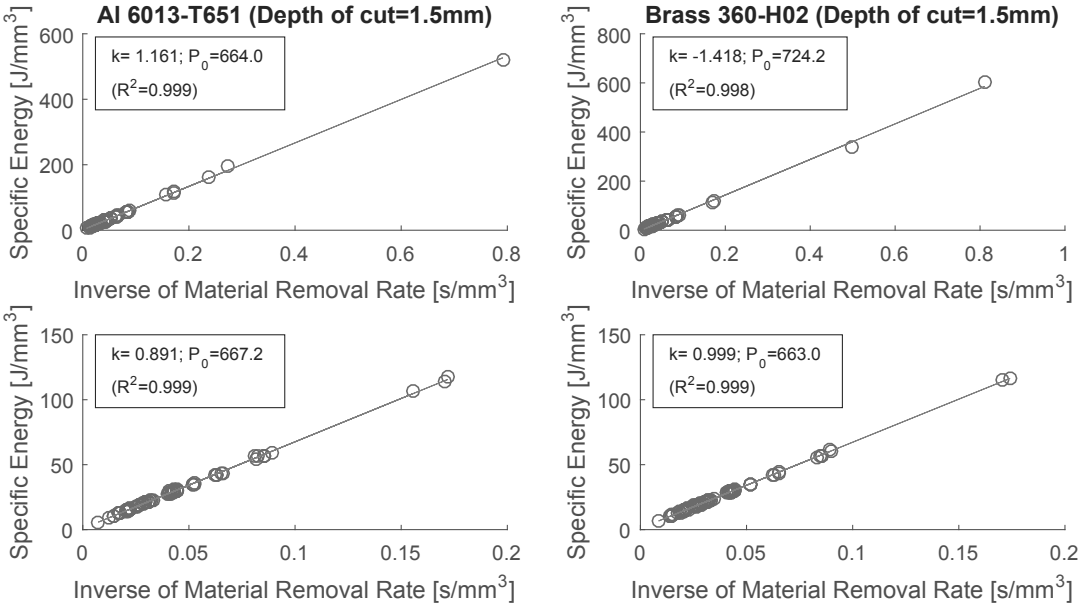

Relationship of specific cutting energy and inverse of material removal rate for 6013-T651 and Brass 360-H02 (Depth of cut =1.5mm). Upper plots include all data while lower plot only includes $MRR^{-1} < 0.2$.